14th World Congress in Computational Mechanics (WCCM)
ECCOMAS Congress 2020
19 – 24 July 2020, Paris, France
F. Chinesta, R. Abgrall, O. Allix and M. Kaliske (Eds)

ADVANCED CONTINUUM MODEL FOR NANO-SIZED THERMOELECTRIC STRUCTURES

JAN SLADEK[1], VLADIMIR SLADEK[1], MIROSLAV REPKA[1] AND ERNIAN PAN[2]

[1]Institute of Construction and Architecture, Slovak Academy of Sciences, 84503 Bratislava, Slovakia
jan.sladek@savba.sk

[2]Computer Modeling and Simulation Group, Department of Civil Engineering, University of Akron, Akron, OH 44325-3905, USA
pan2@uakron.edu

Key words: Size effect, Heat conduction, Mixed FEM, Thermo-electric coupling.
Abstract. The size effect observed in nano-sized structures is considered in the proposed advanced continuum model for heat transfer. It is important for structures, where characteristic microstructural length is comparable with the phonon mean free-path. This feature can be captured by higher-grade continuum models and/or nonlocal modelling of constitutive laws in continuum theories. Both these approaches can be shown equivalent under certain assumptions. The governing equations are given by the PDE with higher-order derivatives than in classical continuum models, with the response of physically conjugated field being proportional to the gradients of primary fields. The variational principle is applied to derive the finite-element formulation for the solution of a thermoelectric 2-d boundary-value problem. Due to higher-order derivatives in gradient theory, it is necessary to use C^1-continuous elements to guarantee the continuity of the derivatives at the element interfaces. Since it is not an easy task, a mixed FEM formulation is developed here.

1 INTRODUCTION

The traditional way of electricity production by fossil fuel combustion should be replaced by a green technology. Thermoelectric materials have a potential to be utilized for this purpose since they are able to convert waste heat directly into electricity by the Seebeck effect [1-4]. However, current thermoelectric materials cannot be utilized for production of electricity because of their low efficiency. The thermoelectric materials should have a high electrical conductivity, low thermal conductivity and high Seebeck coefficient. A high temperature gradients required for generation of a large voltage is occurred only in materials with a low thermal conductivity. Some activities have been devoted to developing thermoelectric composites [5] since it is rather difficult to satisfy above requirements in a single-phase material. Unfortunately, in these approaches the Seebeck coefficient is reduced and electronic contribution to thermal conductivity is growing if electrical conductivity is increased [3]. In the second generation of thermoelectric materials it is needed mainly to understand the carrier transport to reduce mainly the thermal conductivity coefficient. Hochbaum et al. [6] and Boukai et al. [7] have described a way to get optimal thermoelectric properties in nano-structures, where the thermal conductivity is reduced without affecting the high electrical conductivity. In macro-structures the thermal conductivity is dominated by electrons with respect to phonon contribution. However, in nano-sized structures the electronic part of thermal conductivity is less significant [8]. The thermal conductivity is reduced due to scattering of phonons. Electrons are smaller than the size of nanostructures and therefore, the electric conductivity is not reduced in thermoelectric materials. The molecular dynamics (MD) or advanced continuum models are required to describe complex nanoscale systems. Allen [9] has applied the nonlocal theory for the heat flux with temperature gradients.

In this paper an advanced continuum model for heat transfer in nano-sized structures is developed. If the phonon size is comparable to the nano-structure dimension it is needed to consider the size effect in a generalized continuum model. A new continuum model has to replace the classical Fourier heat-conduction model. The Helmholtz form of the kernel function in the nonlocal integral model leads to a differential equation. This idea is similar to the approach applied in the gradient elasticity by Lazar and Polyzos [10].

A reliable and accurate computational tool is needed to solve the general boundary problem described by the higher-order partial differential equations from the new advanced continuum model. The finite element method (FEM) seems to be convenient for this purpose. It has been applied for many problems even in gradient theories [11, 12]. It is the first effort to consider size effect for the heat transfer. The second spatial derivative of temperature is occurred in the constitutive equation of the higher-order heat flux for a coupled thermo-electric problem with nano-sized thermoelectric material structures. Then, the variational principle is applied to derive the governing equations. Due to higher-order derivatives in them, it is needed to use C^1-continuous elements in the FEM. The mixed FEM formulation is then developed to guarantee the required continuities on interfaces of elements. In the mixed FEM, the C^0 continuous interpolation is independently applied to temperature and its gradients. The constraints between temperature and its gradients are satisfied at the Gaussian internal points inside of elements [13]. The size effect on the distribution of temperature and electric potential is discussed via some numerical examples.

2 BASIC EQUATIONS IN GRADIENT THEORY

Thermoelectric properties can be significantly improved in nano-structures [14]. Mainly, the thermal conductivity can be reduced significantly there. The thermal conductivity is reduced due to scattering of phonons if the size of nanostructure is smaller than phonon mean free-path. Since the Fourier heat conduction does not contain a size effect it is needed to consider it in an advanced continuum model. The first effort to consider the size effect is given by Sobolev [15] in the nonlocal heat transport theory. In nonlocal theory the heat flux vector is given by

$$\lambda_i(\mathbf{x}) = -\int_V \alpha(\mathbf{x}-\mathbf{y})\kappa_{ij}(\mathbf{y})\theta_{,j}(\mathbf{y})dV(\mathbf{y}) \ , \tag{1}$$

where the temperature difference is denoted by $\theta = T - T_0$ with the reference temperature T_0, κ_{ij} is the thermal conductivity, and $\alpha(\mathbf{x}-\mathbf{y})$ is a nonlocal kernel function.

The size effect is considered in the nonlocal kernel. It can be selected as

$$\alpha = \frac{1}{4\pi l^2 \rho} \exp(-\rho / l) \tag{2}$$

where $\rho = |\mathbf{x} - \mathbf{y}|$ and l is a characteristic length parameter.

It is easy to show that the kernel function (2) satisfies the Helmholtz equation

$$\left(1 - l^2 \nabla^2\right) \alpha(|\mathbf{x} - \mathbf{y}|) = \delta(\mathbf{x} - \mathbf{y}), \tag{3}$$

where $\delta(\mathbf{x} - \mathbf{y})$ is the Dirac function.

For this special kernel function the integral expression (1) can be converted to the following nonhomogeneous Helmholtz equation

$$\left(1 - l^2 \nabla^2\right) \lambda_i = -\kappa_{ij} \theta_{,j} \text{ or } \left(1 - l^2 \nabla^2\right) \lambda_i = w \tag{4}$$

where w is the volume density of heat source.

If we assume that the constitutive laws for the heat flux λ_i and the higher-grade heat flux m_{ik} (i.e. canonically conjugated fields with $\theta_{,j}$ and $\theta_{,jk}$, respectively) are given as

$$\lambda_i = -\kappa_{ij} \theta_{,j} \ , \tag{5}$$

$$m_{ik} = -l^2 \kappa_{ij} \theta_{,jk} \ , \tag{6}$$

then the governing equation (4) represents the higher-grade heat conduction theory. This theory can be generalized to thermoelectric materials with the following constitutive equations

$$\begin{aligned} \lambda_i &= -\kappa_{ij} \theta_{,j} + \bar{\zeta}_{ij} E_j \, , \\ J_i &= s_{ij} E_j - \zeta_{ik} \theta_{,k} \, , \\ m_{ik} &= -l^2 \kappa_{ij} \theta_{,jk} \ , \end{aligned} \tag{7}$$

where E_j is the electric intensity vector, s_{ij} is the electrical conductivity measured at uniform temperature, and ζ_{ij} and $\bar{\zeta}_{ij}$ are Seebeck and Peltier coefficients, which are calculated via the Seebecks coefficients and absolute temperature as $\bar{\zeta}_{ij} = \zeta_{ij} T$.

For an orthotropic medium in 2-d problem to be considered, the matrix forms of constitutive relationships (7) are given by

$$\begin{pmatrix} J_1 \\ J_2 \end{pmatrix} = \begin{pmatrix} s_{11} & 0 \\ 0 & s_{22} \end{pmatrix} \begin{pmatrix} E_1 \\ E_2 \end{pmatrix} - \begin{pmatrix} \zeta_{11} & 0 \\ 0 & \zeta_{22} \end{pmatrix} \begin{pmatrix} \theta_{,1} \\ \theta_{,2} \end{pmatrix} = [\mathbf{S}]\{\mathbf{E}\} - [\mathbf{Z}] \begin{pmatrix} \theta_{,1} \\ \theta_{,2} \end{pmatrix}, \tag{8}$$

$$\begin{pmatrix} \lambda_1 \\ \lambda_2 \end{pmatrix} = \begin{pmatrix} \bar{\zeta}_{11} & 0 \\ 0 & \bar{\zeta}_{22} \end{pmatrix} \begin{pmatrix} E_1 \\ E_2 \end{pmatrix} - \begin{pmatrix} \kappa_{11} & 0 \\ 0 & \kappa_{22} \end{pmatrix} \begin{pmatrix} \theta_{,1} \\ \theta_{,2} \end{pmatrix} = [\bar{\mathbf{Z}}]\{\mathbf{E}\} - [\boldsymbol{\kappa}] \begin{pmatrix} \theta_{,1} \\ \theta_{,2} \end{pmatrix}. \tag{9}$$

$$\begin{pmatrix} m_{11} \\ m_{21} \\ m_{12} \\ m_{22} \end{pmatrix} = -l^2 \begin{pmatrix} \kappa_{11} & 0 & 0 & 0 \\ 0 & \kappa_{22} & 0 & 0 \\ 0 & 0 & \kappa_{11} & 0 \\ 0 & 0 & 0 & \kappa_{22} \end{pmatrix} \begin{pmatrix} \theta_{,11} \\ \theta_{,21} \\ \theta_{,12} \\ \theta_{,22} \end{pmatrix} = -l^2 [\mathbf{G}]\{\eta\}. \tag{10}$$

Next, the governing equations for thermoelectric materials with the above constitutive equations are derived. The free energy density function ψ contains additional term with higher-grade heat flux with respect to the conventional theory [16]

$$\psi = \frac{1}{2}\lambda_i \theta_{,i} + \frac{1}{2} m_{ik}\theta_{,ik} - \frac{1}{2}\rho c\dot{\theta}\theta + \frac{1}{2} J_i \phi_{,i} \,. \tag{11}$$

Then, the variation of the free energy in a domain V with boundary Γ is given as

$$\delta\psi = \delta\int_V \psi(\theta,\phi)dV = \int_V \left(\lambda_i\delta\theta_{,i} + m_{ik}\delta\theta_{,ik} - \rho c\dot{\theta}\delta\theta + J_i\delta\phi_{,i}\right)dV =$$

$$= -\int_V \left(\lambda_{i,i}\delta\theta + m_{ik,k}\delta\theta_{,i} + J_{i,i}\delta\phi + \rho c\dot{\theta}\delta\theta\right)dV + \int_\Gamma \left(n_i\lambda_i\delta\theta + n_k m_{ik}\delta\theta_{,i} + n_i J_i\delta\phi\right)d\Gamma =$$

$$= -\int_V \left[\left(\lambda_{i,i} - m_{ik,ki} + \rho c\dot{\theta}\right)\delta\theta + J_{i,i}\delta\phi\right]dV + \int_\Gamma \left[n_i\left(\lambda_i - m_{ik,k}\right)\delta\theta + n_k m_{ik}\delta\theta_{,i} + n_i J_i\delta\phi\right]d\Gamma =$$

$$= -\int_V \left[\left(\lambda_{i,i} - m_{ik,ki} + \rho c\dot{\theta}\right)\delta\theta + J_{i,i}\delta\phi\right]dV + \int_\Gamma \left\{\Lambda\delta\theta + P\delta p + Q\delta\phi\right\}d\Gamma \;, \tag{12}$$

where P, Q and Λ are independent boundary densities conjugated to $p = \partial\theta/\partial\mathbf{n}$, ϕ and θ, respectively, and

$$P = n_k n_i m_{ik}\,, \quad Q = n_k J_k\,, \tag{13}$$

$$\Lambda = n_j\left(\lambda_i - m_{ik,k}\right) - \frac{\partial\mu}{\partial\boldsymbol{\tau}} + \sum_c [\![\mu(\mathbf{x}^c)]\!]\,\delta(\mathbf{x}-\mathbf{x}^c) \tag{14}$$

$$\mu = n_k \tau_i m_{ik} \tag{15}$$

with Λ being the heat flux, and n_i and τ_i the Cartesian component of the unit normal and tangent vectors on Γ. If the boundary is not smooth it is needed to consider also the jump at a corner on the oriented boundary contour Γ, defined as $[\![\mu(\mathbf{x}^c)]\!] := \mu(\mathbf{x}^c - 0) - \mu(\mathbf{x}^c + 0)$.

The work of the external "forces" $\left(\bar{\Lambda}, \bar{P}, \bar{Q}\right)$ is given by

$$\delta W = \int_{\Gamma_\Lambda} \bar{\Lambda}\delta\theta d\Gamma + \int_{\Gamma_P} \bar{P}\delta p d\Gamma + \int_{\Gamma_Q} \bar{Q}\delta\phi d\Gamma \,. \tag{16}$$

The Joule heating is created inside the thermoelectric body

$$\delta Q_{gen} = \int_V E_i J_i \delta\theta dV \;. \tag{17}$$

Governing equations are obtained from the first thermodynamic law

$$\delta U + \delta Q_{gen} - \delta W = 0 \,. \tag{18}$$

Substituting (12), (16) and (17) into (18) we obtain the following governing equations

$$\lambda_{i,i}(\mathbf{x}) - m_{ik,ik}(\mathbf{x}) + \rho c\dot{\theta} = E_i J_i\,, \qquad J_{i,i}(\mathbf{x}) = 0\,. \tag{19}$$

3 MIXED FEM FORMULATION

The virtual work for a body with Joule heating inside can be written as

$$\int_V \left(\lambda_i \delta\theta_{,i} + m_{ik}\delta\theta_{,ik} + J_i \delta\phi_{,i} + \rho c\dot{\theta}\delta\theta\right) dV + \int_V E_i J_i \delta\theta dV = \int_{\Gamma_\Lambda} \bar{\Lambda}\delta\theta d\Gamma + \int_{\Gamma_P} \bar{P}\delta p d\Gamma + \int_{\Gamma_Q} \bar{Q}\delta\phi d\Gamma\,. \tag{20}$$

For derivation of the FEM equations, vanishing variations of primary fields have to be considered on the corresponding parts of boundary: $\delta\theta\big|_{\partial V-\Gamma_\Lambda} = 0$, $\delta p\big|_{\partial V-\Gamma_P} = 0$, $\delta\phi\big|_{\partial V-\Gamma_Q} = 0$.

The mixed FEM is developed, where the C^0 continuous interpolation is applied independently for both temperature and temperature gradients. Due to existing constraints between these fields it is needed to satisfy them by collocation at selected internal points of the finite elements [13]. The C^0 continuous interpolation of temperature and electric potential in each element are applied

$$\theta = \mathbf{N}_\theta\left(\xi_1, \xi_2\right)\mathbf{q}_\theta$$
$$\phi = \mathbf{N}_\phi\left(\xi_1, \xi_2\right)\mathbf{q}_\phi\,, \tag{21}$$

where $\mathbf{q}_\theta$ and $\mathbf{q}_\phi$ are the nodal temperature and electric potential, respectively, with $\boldsymbol{N}_\theta$ and $\boldsymbol{N}_\phi$ being their shape functions.

The normal derivatives of the temperature, electric intensity vector and temperature gradients are obtained from (21) as:

$$p = \left(n_1\partial_1 + n_2\partial_2\right)\theta = \mathbf{B}_s(\xi_1, \xi_2)\mathbf{q}_\theta$$
$$-\mathbf{E} = -\begin{bmatrix} E_1 \\ E_2 \end{bmatrix} = \begin{bmatrix} \partial_1 \\ \partial_2 \end{bmatrix}\phi = \mathbf{B}_\phi(\xi_1, \xi_2)\mathbf{q}_\phi\;, \qquad \boldsymbol{\varepsilon} = \begin{bmatrix} \theta_{,1} \\ \theta_{,2} \end{bmatrix} = \begin{bmatrix} \partial_1 \\ \partial_2 \end{bmatrix}\theta = \mathbf{B}_\theta(\xi_1, \xi_2)\mathbf{q}_\theta\;, \tag{22}$$

with $\mathbf{B}_\phi(\xi_1, \xi_2) = \mathbf{B}_\theta(\xi_1, \xi_2)$.

In the mixed FEM with temperature gradients it is needed to have also an independent approximation of $\boldsymbol{\varepsilon}$:

$$\hat{\boldsymbol{\varepsilon}}^{In} = \mathbf{A}_\varepsilon\left(\xi_1, \xi_2\right)\boldsymbol{\alpha}\,, \tag{23}$$

where $\boldsymbol{\alpha}$ are undetermined coefficients defined separately for each component of the temperature gradient.

Now, the 4-node quadrilateral element are considered with the polynomial function matrix

$$\mathbf{A}_\varepsilon\left(\xi_1, \xi_2\right) = \begin{bmatrix} 1 & \xi_1 & \xi_2 & \xi_1\xi_2 \end{bmatrix}. \tag{24}$$

The collocation of two-independent approximations of temperature gradients, $\boldsymbol{\varepsilon}$ given by (22) and (23), is performed at Gauss quadrature points $\boldsymbol{\xi}^c = (\xi_1^c, \xi_2^c)$

$$\mathbf{A}_\varepsilon(\boldsymbol{\xi}^c)\boldsymbol{\alpha} = \mathbf{B}_\theta(\boldsymbol{\xi}^c)\mathbf{q}_\theta\,. \tag{25}$$

It follows directly from (25) that

$$\boldsymbol{\alpha} = \mathbf{A}_\varepsilon^{-1}(\boldsymbol{\xi}^c)\mathbf{B}_\theta(\boldsymbol{\xi}^c)\mathbf{q}_\theta\;. \tag{26}$$

The final expression for the independent approximation of $\boldsymbol{\varepsilon}$ is given by

$$\hat{\boldsymbol{\varepsilon}}^{In} = \mathbf{A}_{\varepsilon}(\xi_1, \xi_3)\mathbf{L}\mathbf{q}_{\theta}\,, \tag{27}$$

where $\mathbf{L} = \mathbf{A}_{\varepsilon}^{-1}(\boldsymbol{\xi}^c)\mathbf{B}_{\theta}(\boldsymbol{\xi}^c)$.

Finally, the derivatives of the temperature gradients $\boldsymbol{\eta}$ are given as

$$\hat{\boldsymbol{\eta}}^{In} = \begin{bmatrix} \partial_1 \\ \partial_2 \end{bmatrix} \hat{\boldsymbol{\varepsilon}}^{In} = \begin{bmatrix} \partial_1 \\ \partial_2 \end{bmatrix} \mathbf{A}_{\varepsilon}\left(\xi_1, \xi_2\right)\boldsymbol{\alpha} = \mathbf{A}_{\varepsilon}^{*}\left(\xi_1, \xi_2\right)\boldsymbol{\alpha} = \mathbf{A}_{\varepsilon}^{*}\left(\xi_1, \xi_2\right)\mathbf{L}\mathbf{q}_{\theta}\,. \tag{28}$$

Substituting above approximations into the functional (20) and taking into account that variations $\left\{\delta\mathbf{q}_{\phi}\right\}$ and $\left\{\delta\mathbf{q}_{\theta}\right\}$ are arbitrary, we obtain the following two nonlinear ordinary differential equations

$$\begin{aligned}
&-\int_V \mathbf{B}_{\theta}^T(\boldsymbol{\xi})\bar{\mathbf{Z}}\mathbf{B}_{\phi}(\boldsymbol{\xi})\left\{\mathbf{q}_{\phi}^{(k)}\right\}dV - \int_V \left(\mathbf{B}_{\theta}^T(\boldsymbol{\xi})\left[\boldsymbol{\kappa}\right]\mathbf{B}_{\theta}(\xi_1, \xi_2) + \mathbf{L}^T\mathbf{A}_{\varepsilon}^{*T}(\boldsymbol{\xi})l^2\mathbf{G}\mathbf{A}_{\varepsilon}^{*}(\boldsymbol{\xi})\mathbf{L}\right)\left\{\mathbf{q}_{\theta}^{(k)}\right\}dV - \\
&-\int_V \mathbf{N}_{\theta}^T(\boldsymbol{\xi})\rho c\mathbf{N}_{\theta}(\boldsymbol{\xi})\left\{\dot{\mathbf{q}}_{\theta}^{(k)}\right\}dV = \int_{\Gamma_\Lambda} \mathbf{N}_{\theta}^T\bar{\Lambda}d\Gamma + \int_{\Gamma_p} \mathbf{B}_s^T\bar{P}d\Gamma - \\
&-\int_V \mathbf{N}_{\theta}^T(\boldsymbol{\xi})\left\{\mathbf{q}_{\phi}^{(k-1)}\right\}^T\mathbf{B}_{\phi}^T(\boldsymbol{\xi})\left(\mathbf{S}\mathbf{B}_{\phi}(\boldsymbol{\xi})\left\{\mathbf{q}_{\phi}^{(k-1)}\right\} + \left[\mathbf{Z}\right]\mathbf{B}_{\theta}(\xi_1, \xi_2)\left\{\mathbf{q}_{\theta}^{(k-1)}\right\}\right)dV
\end{aligned} \tag{29}$$

$$\int_V \mathbf{B}_{\phi}^T(\boldsymbol{\xi})\left(\mathbf{S}\mathbf{B}_{\phi}(\boldsymbol{\xi})\left\{\mathbf{q}_{\phi}^{(k)}\right\} + \left[\mathbf{Z}\right]\mathbf{B}_{\theta}(\xi_1, \xi_2)\left\{\mathbf{q}_{\theta}^{(k)}\right\}\right)dV = -\int_{\Gamma_Q} \mathbf{N}_{\phi}^T\bar{Q}d\Gamma\,, \tag{30}$$

which should be solved iteratively, with starting values $\left\{\mathbf{q}_{\phi}^{(0)}\right\} = \left\{0\right\}$, $\left\{\mathbf{q}_{\theta}^{(0)}\right\} = \left\{0\right\}$.

4 NUMERICAL REULTS

An infinite strip is analysed with the following boundary conditions (Fig. 1):

$$\theta(0) = T_0 - T_0 = 0\,,\quad \theta(L) = T_L - T_0\,,\quad \theta'(0) = 0 = \theta'(L)\,,\quad \phi(0) = \phi_0\,,\quad \phi(L) = \phi_L\,.$$

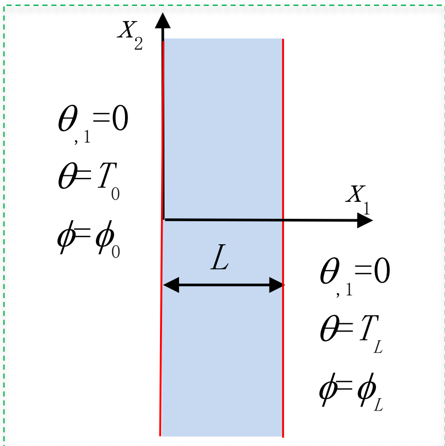

Figure 1: An infinite strip with boundary conditions on x_1=0 and x_1=L.

Isotropic material properties are considered with ζ-Seebeck coefficient, *s*-electric current conductivity and κ-heat conduction coefficient, where the constitutive relationships are simplified to

$$J_i = -s\phi_{,i} - \alpha s\theta_{,i}$$

$$\lambda_i = -\alpha sT\phi_{,i} - (\kappa + \alpha^2 sT)\theta_{,i} = \alpha TJ_i - \kappa\theta_{,i} \ .$$

The thermoelectric material, Bi_2Te_3, is considered in the numerical example. It has the following material constants [17] with isotropic properties:

$$s = 1.1\times10^5 Am/V \ , \qquad \alpha = \zeta / s = 2\times10^{-4}\,\mathrm{V}^2/KAm \ , \qquad \kappa = 1.6W/Km \ . \qquad (31)$$

Characteristic length for the selected material structure is $l = 5\times10^{-9}m$.
This 1-D problem can be solved numerically as a 2-D problem with the height of the strip *H*=5*L*. Numerical results for the induced electric potential for various ratio *l/L* are presented in Fig. 2. One can observe that with increasing ratio *l/L* the induced potential grows. It is due to the reduced thermal conduction value in the smaller structures.

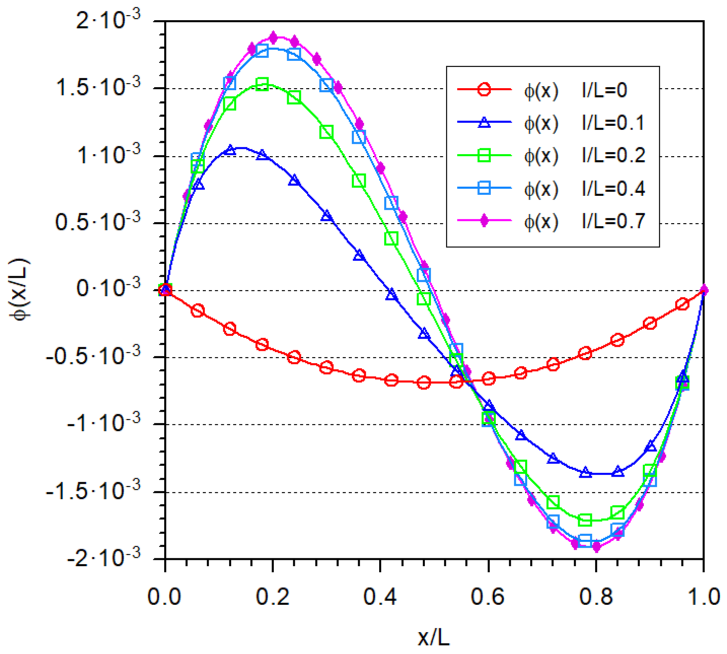

Figure 2: Variation of electric potential vs. the strip width

The thermoelectric conversion efficiency is given by the dimensionless figure of merit ZT [18]:

$$ZT = \frac{\alpha^2 sT}{\kappa} \ .$$

In the higher-grade theory, the value of heat conduction coefficient can be assessed as $\kappa - \kappa(l/L)^2 < \kappa$, where L is a characteristic linear dimension of the thermoelectric body.

Hence, the assessment of the figure of merit of thermoelectric conversion efficiency in higher-grade thermoelectricity overcomes that in classical thermoelectricity

$$ZT = \frac{\alpha^2 sT}{\kappa - \kappa(l/L)^2} > \frac{\alpha^2 sT}{\kappa}.$$

The variation of merit of conversation efficiency along the strip thickness is presented in Fig. 3. One can observe a significant enhancement on the ZT parameter if the thickness is decreasing.

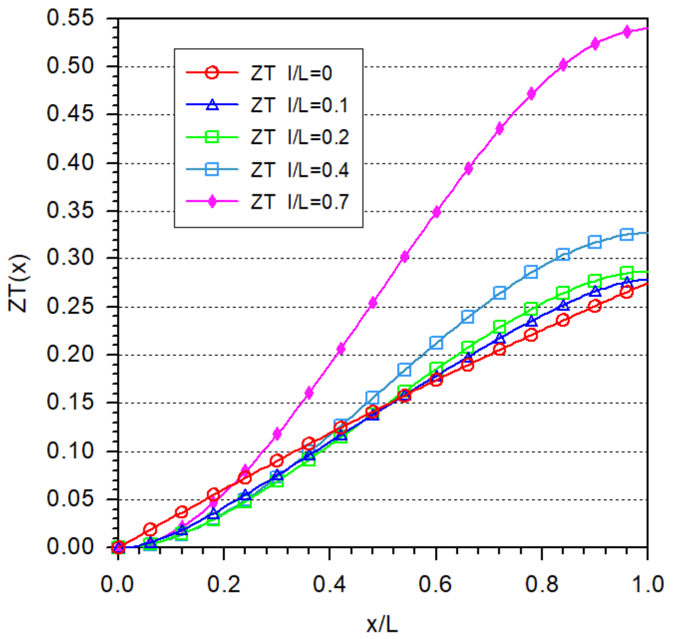

Figure 3: Variation of conversion efficiency *ZT* with different ratio l/L

5 CONCLUSIONS

Optimal thermoelectric properties with a high conversion efficiency can be obtained in nano-structures, where the thermal conductivity is reduced without affecting the high electrical conductivity. A new continuum model has to replace the classical Fourier heat conduction model in nano-sized structures, where a size effect is observed.

The expression for the higher-grade heat flux is derived from the nonlocal models with a special kernel function. Then, the principle of the virtual works is applied to derive the governing equations. These PDEs have higher-order derivatives than in classical continuum models with the response of physically conjugated field being proportional to gradients of primary fields. The FEM equations are derived too. Due to higher-order derivatives in gradient theory, the mixed FEM formulation is developed here. The C^0 continuous interpolation is independently applied for temperature and its gradients.

The influence of the size effect is investigated for an infinite strip (1-D problem). The conversion efficiency parameter is significantly enhanced if the thickness of the strip is reduced.

ACKNOWLEDGEMENT

The authors acknowledge the support by the Slovak Science and Technology Assistance Agency registered under number SK-CN-RD-18-0005 and VEGA-2/0061/20.

REFERENCES

[1] Callen, H.B. *Thermodynamics: An Introduction to the Physical Theories of Equilibrium Thermostatics and Irreversible Thermodynamics*. Wiley (1960).
[2] Nagy, P.B. and Nayfeh, A.H. On the thermoelectric magnetic field of spherical and cylindrical inclusions. *J. Appl. Phys.* (2000) **87**: 7481.
[3] Minnich, A.J., Dresselhaus, M.S., Ren, Z.F. and Chen, G. Bulk nanostructured thermoelectric materials: current research and future prospects. *Energy Environ. Sci.* (2009) **2**: 466-479.
[4] Bies, W.E., Radtke, R.J. and Ehrenreich, H. Thermoelectric properties of anisotropic semiconductors. *Phys. Rev. B* (2002) 65: 085208.
[5] Cao, Y.Q., Zhao, X.B., Zhu, T.J., Zhang, X.B. and Tu, J.P. Syntheses and thermoelectric properties of Bi(2)Te(3)/Sb(2)Te(3) bulk nanocomposites with laminated nanostructure. *Appl. Phys. Lett.* (2008) **2**: 143106-1–3.
[6] Hochbaum, A.I., Chen, R.K., Delgado, R.D., Liang, W.J., Garnett, E.C., Najarian, M., Majumdar, A., and Yang, P.D. Enhanced thermoelectric performance of rough silicon nanowires. *Nature* (2008) 451: 163-167.
[7] Boukai, A.I., Bunimovich Y., Tahir-Kheli, J., Yu J.K., Goddard, W.A. and Heath, J.R. Silicon nanowires as efficient thermoelectric materials. *Nature* (2008) 451: 168-171.
[8] Stojanovic, N., Maithripala, D.H.S., Berg, J.M. and Holtz, M. Thermal condictivity in metallic nanostructures at high temperature: electrons, phonons, and the Wiedemann-Franz law. *Phys. Rev. B* (2010) 82: 075418.
[9] Allen, PB. Size effects in thermal conduction by phonons. *Phys. Rev. B* (2014) 90: 054301.
[10] Lazar, M. and Polyzos, D. (2015) On non-singular crack fields in Helmholtz type enriched elasticity theories, *Int. J. Solids Struct.* (2015) 62: 1-7.
[11] Sladek, J., Sladek, V., Stanak, P., Zhang, Ch. and Tan C.L. Fracture mechanics analysis of size-dependent piezoelectric solids. *Int. J. Solids Struct.* (2017) 113: 1-9.
[12] Sladek, J., Sladek, V., Repka, M., Schmauder, S. Gradient theory for crack problems in quasicrystals. *Eur. J. Mechanics / A Solids* (2019) 77: 103813.
[13] Dong, L. and Atluri, S.N. A simple procedure to develop efficient & stable hybrid/mixed elements, and Voronoi cell finite elements for macro- & micromechanics. *CMC: Computers, Materials & Continua* (2011) 24: 61–104.
[14] Hicks, L. and Dresselhaus, M.S. Thermoelectric figure of merit of a one-dimensional conductor. *Phys. Rev. B* (1993) **47**: 16631.

[15] Sobolev, S. Equations of transfer in non-local media. *Int. J. Heat Mass Transf.* (1994) 37: 2175–2182.
[16] Wang, X., Pan, E. and Albrecht, J.D. Role of material property gradient and anisotropy in thermoelectric materials. *New Journal of Physics* (2008) 10: 083019.
[17] Yang, Y., Gao, C., Li, J. The effective thermoelectric properties of core-shell composites. *Acta Mechanica* (2014) 225: 1211-1222.
[18] Tritt, T.M., Boettner, M., Chen, L. Thermoelectrics: direct solar termal energy conversation. *MRS Bulletin* (2008) 33: 366-368.